DETERMINATION OF A NONLINEAR COEFFICIENT IN A TIME-FRACTIONAL DIFFUSION EQUATION

Mustafa Zeki[1], Ramazan Tinaztepe[2], Salih Tatar[3], and Suleyman Ulusoy[4]

[1]American University of the Middle East
[2]Imam Abdulrahman Bin Faisal University
[3]Alfaisal University
[4]American University of Ras Al Khaimah

September 5, 2022

Abstract

Direct and inverse problems for a nonlinear time fractional equation are studied. It is proved that the direct problem has a unique weak solution and the solution depends continuously on the nonlinear coefficient. Then it is shown that the inverse problem has a quasi-solution. The direct problem is solved by method of lines using an operator approach. A quasi-Newton optimization method is used for the numerical solution to the inverse problem. Tikhonov regularization is used to overcome the ill-posedness of the inverse problem. Numerical examples with noise free and noisy data illustrate applicability and accuracy of the proposed method to some extent.

DETERMINATION OF A NONLINEAR COEFFICIENT IN A TIME-FRACTIONAL DIFFUSION EQUATION

MUSTAFA ZEKİ, RAMAZAN TINAZTEPE, SALİH TATAR, AND SÜLEYMAN ULUSOY

Abstract. Direct and inverse problems for a nonlinear time fractional equation are studied. It is proved that the direct problem has a unique weak solution and the solution depends continuously on the nonlinear coefficient. Then it is shown that the inverse problem has a quasi-solution. The direct problem is solved by method of lines using an operator approach. A quasi-Newton optimization method is used for the numerical solution to the inverse problem. Tikhonov regularization is used to overcome the ill-posedness of the inverse problem. Numerical examples with noise free and noisy data illustrate applicability and accuracy of the proposed method to some extent.

Keywords. Fractional diffusion, Inverse problem, Quasi-solution, Existence and uniqueness, Method of lines.
AMS Subject Classifications. 34A12, 35R11, 35R30, 65F22, 65M32.

1. Introduction

In the last years, different approaches are given for modeling diffusion in the media of fractal geometry, [1]-[10]. Such an approach is based on employing fractional differential equations and we use this approach in this paper. For the completeness, we give a brief background. One-dimensional mass transport due to diffusion is given by

$$\frac{\partial u}{\partial t} = -\frac{\partial}{\partial x}\left(J_u\right), \tag{1.1}$$

where J_u is the diffusive mass flux. For Fickian diffusion, it is given by

$$J_u = -D^{(m)}\frac{\partial u}{\partial x}, \tag{1.2}$$

where $D^{(m)}$ is the diffusion coefficient. By introducing the new non-dimensional variables $X = \dfrac{x}{x_0}$, $\tau = \dfrac{x}{x_0}$, $U = \dfrac{u}{u_0}$, where x_0, t_0 and u_0 are the characteristic scales, equations (1.1) and (1.2) can be given in the non-dimensional form as follows:

$$\frac{1}{t_0}\frac{\partial U}{\partial \tau} = \frac{1}{x_0^2}\frac{\partial}{\partial X}\left(D^{(m)}\frac{\partial U}{\partial X}\right). \tag{1.3}$$

If $x_0 = t_0$, then equations (1.1) and (1.2) preserve their original form. However many experiments with fractal objects show that this correlation does not hold. In this case, it is proved that the-mean square displacement of a random walker $< x^2 > \sim\ t^{\frac{2}{2+\theta}}$, where θ is the index of the anomalous diffusion. Then we have the correlation $< x_0^2 > \sim\ t_0^{\frac{2}{2+\theta}}$. It is clear that there are many expressions for the mass flux that corresponds to that correlation. For example, the diffusion coefficient

may be defined as $D^{(m)}(x) = D_f x^{-\theta}$, where $D_f \equiv$ constant is the effective diffusion coefficient. Then we have the following diffusion equation

$$\frac{\partial u}{\partial t} = \frac{\partial}{\partial x}\left(D_f x^{-\theta}\frac{\partial u}{\partial x}\right). \tag{1.4}$$

As another example, the mass flux may be taken proportional to the fractional derivative of concentration with respect to spatial coordinate of the order $\theta+1$. In this case, the obtained mass flux is doubtful since the order of the corresponding diffusion equation is greater than 2. For this reason, the following expression for the mass flux is considered:

$$J_u = D_f \partial_t^{1-\beta}\left(\frac{\partial^\gamma u}{\partial x^\gamma}\right), \beta > 0, \gamma < 1, \tag{1.5}$$

where β and γ are the order of the temporal and spatial fractional derivatives respectively. In (1.5), ∂_t^β and ∂_x^γ are spatial and temporal Caputo fractional derivatives and are defined as follows:

$$\partial_x^\gamma u(x,t) = \frac{\partial^\gamma u(x,t)}{\partial x^\gamma} = \frac{1}{\Gamma(1-\gamma)}\int_0^x (x-\xi)^{-\gamma}\frac{\partial u(\xi,t)}{\partial \xi}d\xi,$$
$$\partial_t^\beta u(x,t) = \frac{\partial^\beta u(x,t)}{\partial t^\beta} = \frac{1}{\Gamma(1-\beta)}\int_0^t (t-\xi)^{-\beta}\frac{\partial u(x,\xi)}{\partial \xi}d\xi,$$

where $\Gamma(\cdot)$ is the Gamma function. We note that there is another kind of fractional derivative that is used frequently called the Riemann-Lioville fractional derivative defined by

$${}^R\partial_t^\beta u(x,t) = \frac{1}{\Gamma(1-\beta)}\frac{\partial}{\partial t}\int_0^t (t-\xi)^{-\beta}u(x,\xi)d\xi.$$

These two fractional derivatives agree when the initial condition is zero. Kilbas et al [11] and Podlubny [12] can be referred for further properties of the Caputo and Riemann-Lioville fractional derivatives. Since the initial condition is zero in our problem, any result found in the literature for one of these hold for the other one.

Then by putting the definitions of the Caputo derivatives in (1.5), we have:

$$\frac{\partial u}{\partial t} = \frac{\partial}{\partial x}\left(D_f \partial_t^{1-\beta}\frac{\partial^\gamma u}{\partial x^\gamma}\right), \tag{1.6}$$

where γ and β are coupled such that $< x_0^2 > \sim t_0^{\frac{2}{2+\theta}}$ is satisfied. It can be shown that the correlation $t_0 = x_0^{\frac{1+\gamma}{\beta}}$ holds. Then we conclude that $\theta + 2 = \dfrac{1+\gamma}{\beta}$. By applying the fractional integral operator to both sides of (1.6), we find the following useful form:

$$\frac{\partial^\beta u}{\partial t^\beta} = \frac{\partial}{\partial x}\left(D_f \frac{\partial^\gamma u}{\partial x^\gamma}\right). \tag{1.7}$$

This equation can be found in many papers on the diffusion phenomena in the chaotic migration of the particles and anomalous contaminant diffusion from a fracture into a porous rock matrix with an alteration zone bordering the fracture,

see [13]-[17] and some of the references cited therein. Assuming the porous medium has a comb-like structure of fractal geometry, $\gamma = 1$ case is also considered in the mathematical literature, see [18, 19]. We refer the readers to [20] for more details and motivation regarding the equation (1.7).

When a porous medium equation is considered, the pressure is taken to be a monotone function of the concentration u. In this case, by using the corresponding Darcy's Law and the continuity equation, the following nonlinear equation is obtained:

$$u_t + \nabla \cdot (d(u)\nabla u) = 0. \tag{1.8}$$

Equation (1.8) is also known as the Richards' equation in the hydrology [21].

For the convenience of the reader, we present the main steps of the derivation of the governing equation by following [22]. If the fluid particles are trapped in some region for several periods of time $s_1, \cdots, s_n$ then the continuity equation becomes

$$u_t = -\sum_{i=1}^{n} w_i \nabla \cdot q(x, t - s_i), \tag{1.9}$$

where w_i are some weights. If we take $w_i = w(s_i)\Delta s_i$ with $\Delta s_i = s_i - s_{i-1}$ for some weight density $w = w(s)$, and take limit as $n \to \infty$, (1.9) becomes

$$u_t = -\int_0^t w(t - s)\nabla \cdot q(x, s)\, ds. \tag{1.10}$$

Equation (1.10) accounts for the fluid particles that can be trapped for any period of time. The amount of flux of the particles that wait for the time equals $w(s)$. Using the choice of [22] for w, we arrive at

$$u_t = -\frac{1}{\Gamma(\beta)} \frac{\partial}{\partial t} \int_0^t (t - s)^{\beta - 1} \nabla \cdot q(x, s)\, ds = -{}^R\partial_t^{1-\beta} \nabla \cdot q. \tag{1.11}$$

If we apply the Riemann-Lioville fractional operator $I_t^{1-\beta}$ to both sides of (1.11) and take into account the composition formula for the functions with vanishing initial conditions we have:

$$\frac{\partial^\beta}{\partial t^\beta} u = \nabla \cdot (d(u)\nabla u)\,. \tag{1.12}$$

Equation (1.12) is also called generalized Richards equation [23] and can be found in may papers. In [23], (1.12) is solved numerically and fitted the solution to data on horizontal water transport. The numerical solution is also studied by some authors, see [24]-[27]. In [28], magnetic resonance imaging is employed to study water ingress in fine zeolite powders compacted by high pressure. The measured moisture profiles indicate sub-diffusive behavior with a spatio-temporal scaling variable $\eta = \dfrac{x}{t^{\gamma/2}}$. Equation (1.12) is used to analyze the data, and an expression that yields the moisture dependence of the generalized diffusivity is derived and applied to their measured profiles. In [29], the authors use a time-fractional diffusion equation for modeling the probability density function of displacements. In [30], the author describes a method of approximating equations with the Erdelyi-Kober

fractional operator which arise in mathematical descriptions of anomalous diffusion. A theorem is also proved on the exact form of the approximating series and provide an illustration by considering the fractional porous-medium equation used to model moisture diffusion in building materials. The authors look for self-similar solutions for the equation (1.12) in [31]. The resulting similarity equations are of nonlinear integro-differential type. They approximate these equations by an expansion of the integral operator and by looking for solutions in a power function form. Several applications of the equation (1.12) are presented in [32]. Recently, there has been a growing interest in inverse problems with fractional derivatives. These problems are physically and practically very important. We list some of the important references, [33]-[46]. In the current paper, we study an inverse coefficient problem for the nonlinear time-fractional diffusion equation (1.12). The difference of the current study from the references [33]-[46] is that the unknown of the inverse problem is non-linear, i.e depends on the solution u. This is a relatively new topic and there are only few works, see [47]-[49]. In [47], the unknown coefficient depends on the gradient of the solution and belongs to a set of admissible coefficients. The authors prove that the direct problem has a unique solution and show the continuous dependence of the solution of the corresponding direct problem on the unkown coefficient. Then, existence of a quasi-solution of the inverse problem is obtained in the appropriate class of admissible coefficients. In [48], the authors study the numerical solutions of the direct and the inverse problems in [47] and mention about an application of the governing equation in the materials sciences. An inverse problem for the nonlinear time-fractional diffusion equation (1.12) is studied in [49]. In this paper, the authors prove that the direct problem has a unique solution. Existence of a quasi-solution is also proved. However neither the uniqueness of the solution is proved nor the direct and the inverse problems solved numerically. In this context, this study can be regarded as continuation of the series of work in [49] and the works mentioned above on fractional inverse problems. It is also worth mentioning that some inverse problems are studied for $\beta = 1$ in (1.12). For example; in [50], the determination of the unknown coefficient $d(u)$ from over-specified data measured at the boundary is studied. The inverse problem is reformulated as an auxiliary inverse problem and it is shown that this auxiliary problem has at least one solution in a specified admissible class. Finally, the auxiliary problem is approximated by an associated identification problem and some numerical results are presented. In [51], an operator approach is improved by an input-output mapping and it is shown that the mapping is isotonic. This result is used to derive a uniqueness result for the inverse problem.

This paper is organized as follows: In the next section, we formulate the direct and the inverse problems. Existence and uniqueness for the direct and the inverse problems are discussed in Section 3. The numerical solutions of the direct and the inverse problems are studied in Section 4 and in Section 5, respectively. The conclusions and possible directions on the problem are given in Section 6.

2. Formulation of the direct and the inverse problems

In this section, we formulate the direct and the inverse problems. First, we consider the following problem:

$$\begin{cases} \dfrac{\partial^\beta u}{\partial t^\beta} = \nabla \cdot (d(u)\nabla u) + f(x,y,t), (x,y,t) \in \Omega_T, \\ u(x,y,t) = 0, \qquad (x,y,t) \in \Gamma_{3T} \cup \in \Gamma_{4T}, \\ d(u)u_y(x,y,t) = g_1(x,t), (x,y,t) \in \Gamma_{1T}, \\ d(u)u_x(x,y,t) = g_2(y,t), (x,y,t) \in \Gamma_{2T}, \\ u(x,y,0) = 0, \qquad\qquad (x,y) \in \bar{\Omega}, \end{cases} \tag{2.1}$$

where β is the order of the Caputo fractional time derivative, $\Omega := (0,1) \times (0,1)$, $\Omega_T := \Omega \times (0,T)$, $\Gamma_{iT} := \Gamma_i \times (0,T), i = 1,2,3,4$ and $T > 0$ is a final time. We assume that Ω is a bounded simply connected domain with a piece-wise smooth boundary $\partial\Omega = \Gamma_1 \cup \Gamma_2 \cup \Gamma_3 \cup \Gamma_4$, $\Gamma_i \cap \Gamma_j = \emptyset$, $i \neq j$. We define $\Gamma_i, i = 1,2,3,4$ as follows:

$$\Gamma_1 := (0,1) \times \{1\}, \Gamma_2 := \{1\} \times (0,1),$$
$$\Gamma_3 := (0,1) \times \{0\}, \Gamma_4 := \{0\} \times (0,1).$$

For given inputs β, $d(u)$, $f(x,y,t)$, $g_1(x,t)$ and $g_2(y,t)$, the problem (2.1) is called the direct problem. Next, we define the class of admissible coefficients and the weak solution of the problem (2.1). We note that, throughout the paper while, $\|\cdot\|$ and $\langle , \rangle$ denote the usual $L^2(\Omega)$ norm and inner product respectively, $\|\cdot\|_X$ denotes the norm in a Hilbert space X. $C(l)$ denotes the set of continuous functions defined on l.

Definition 2.1. Let l be a closed interval. A set $\mathbb{D}$ satisfying the following conditions is called the class of admissible coefficients for the problem (2.1) :

$$d \in C(l), \quad c_0 \leq d(s) \leq c_1, \forall\, s \in l, \tag{2.2}$$

$$\big(d(u_1)\nabla u_1 - d(u_2)\nabla u_2\big) \cdot \nabla(u_1 - u_2) \geq c_2 ||\nabla(u_1 - u_2)||^2, \forall\, u_1, u_2 \in H_0^1(\Omega), \tag{2.3}$$

where c_0, c_1, c_2 are positive constants.

Definition 2.2. A weak solution of the problem (2.1) is a function $u \in S^\beta(\Omega_T) := L^2\left(0,T; H_0^1(\Omega)\right) \cap W_2^\beta\left(0,T; L^2(\Omega)\right)$ such that the following integral identity holds for a.e. $t \in [0,T]$:

$$\begin{aligned} &\int_\Omega \frac{\partial^\beta u}{\partial t^\beta}\, v\, dx\, dy + \int_\Omega d\,(u)\, \nabla u \cdot \nabla v\, dx\, dy \\ &\qquad = \int_\Omega f\, v\, dx\, dy + \int_{\Omega_3} g_1\, v\, dx\, dy + \int_{\Omega_4} g_2\, v\, dx\, dy, \end{aligned} \tag{2.4}$$

for each $v \in S^\beta(\Omega_T)$, where

$$W_2^\beta(0,T) := \left\{ u \in L^2[0,T] : \frac{\partial^\beta u}{\partial t^\beta} \in L^2[0,T] \,\text{and}\, u(0) = 0 \right\},$$

is the fractional Sobolev space of order β. We note that $S^{\beta}(\Omega_T)$ is a Banach space with the norm :

$$\|u\|_{S^{\beta}(\Omega_T)} = \left(\|u\|^2_{W_2^{\beta}(0,T;L^2(\Omega))} + \|u\|^2_{L^2\left(0,T;H_0^1(\Omega)\right)} \right)^{\frac{1}{2}}.$$

We regard $u(x,y,t)$ as a mapping from $t \in (0,T)$ to $L^2(\Omega)$ and write $u(t) = u(\cdot,\cdot,t)$.

A weak solution of the problem (2.1) is also defined as a solution of the following abstract operator equation

$$Lu + Au = F, \tag{2.5}$$

where $Lu := \left\langle \hat{L}u, v \right\rangle$, $\hat{L}u := \dfrac{\partial^{\beta} u}{\partial t^{\beta}}$, $\hat{L} : D(\hat{L}) \subset V \to V^*$ with the domain $D(\hat{L}) = \left\{ u \in V : \dfrac{\partial^{\beta} u}{\partial t^{\beta}} \in V^* \right\}$, $V := L^2\left(0,T;H_0^1(\Omega)\right)$, the nonlinear operator $A : V \to V^*$ is defined by

$$\left\langle Au, v \right\rangle := \int\limits_{\Omega} \frac{\partial^{\beta} u}{\partial t^{\beta}} \, v \, dx \, dy + \int\limits_{\Omega} d\,(u) \, \nabla u \cdot \nabla v \, dx \, dy, \tag{2.6}$$

and F on V is defined by

$$\left\langle F, v \right\rangle := \int\limits_{\Omega} f \, v \, dx \, dy + \int_{\Omega_3} g_1 \, v \, dx \, dy + \int_{\Omega_4} g_2 \, v \, dx \, dy. \tag{2.7}$$

The inverse problem here consists of determining the pair of functions $\{u(x,y,t), d(u)\}$ from the problem (2.1) by means of the additional data $u(x,y,t) = \hat{g}_1(x,t), (x,y,t) \in \Gamma_{1T}$ and $u(x,y,t) = \hat{g}_2(y,t), (x,y,t) \in \Gamma_{2T}$. For the consistency of the additional data with the data of (2.1) on Γ_{1T} and Γ_{2T}, it is assumed that $d(\hat{g}_1(x,t))(\hat{g}_1)_y(x,y,t) = g_1(x,t)$ on Γ_{1T} and $d(\hat{g}_2(x,t))(\hat{g}_2)_y(x,y,t) = g_1(x,t)$ on Γ_{2T}.

We denote the solution of the direct problem (2.1) for a given function $d \in \mathbb{D}$ by $u(x,y,t;d)$. If the function $u(x,y,t;d)$ also satisfies the additional data above, it is called a strict solution of the inverse problem. Now, we reformulate the inverse problem. For this purpose, we introduce the input-output map :

$$\Phi(d) := u(x,y,t;d)|_{\Gamma_{3T} \times \Gamma_{4T}} := \left(u(x,y,t;d)|_{\Gamma_{3T}}, u(x,y,t;d)|_{\Gamma_{4T}} \right), \tag{2.8}$$

where $\Phi : L^2(\Omega_T) \to L^2(\Gamma_{3T}) \times L^2(\Gamma_{4T})$. Then the inverse problem is defined as a solution of the following operator equation :

$$\Phi(d) = g, \;\; g = (\hat{g}_1(x,t), \hat{g}_2(y,t)) \in L^2(\Gamma_{3T}) \times L^2(\Gamma_{4T}). \tag{2.9}$$

However, due to measurement errors in practice exact equality in (2.9) is usually not achieved. Hence, one needs to introduce the following auxiliary (cost) functional :

$$I(d) := \int_0^T \int\limits_{\Gamma_3} \left| u(x,y,t;d) - \hat{g}_1(x,t) \right|^2 dx \, dt + \int_0^T \int\limits_{\Gamma_4} \left| u(x,y,t;d) - \hat{g}_2(y,t) \right|^2 dy \, dt, \tag{2.10}$$

and consider the following minimization problem

$$I(\hat{d}) = \min_{d \in \mathbb{D}} I(d). \tag{2.11}$$

A solution of the minimization problem (2.11) is called a quasi-solution (or approximate solution) of the inverse problem . Evidently, if $I(\hat{d}) = 0$ then the quasi-solution $\hat{d}$ is also a strict solution of the inverse problem. Analyses of the direct and inverse problems are given in the following section.

3. Analysis of the direct and the inverse problems

In this section, we analyze both the direct and the inverse problems. The theoretical aspect of the direct problem (2.1) is studied in [49]. In this study, the authors prove that the direct problem (2.1) is well-posed in the sense of Hadamard. For the sake of the reader we provide some relevant results from [49]. The following theorems state that the direct problem (2.1) has a unique weak solution and the solution depends continuously on the coefficient $d(u)$. We refer the readers to [49] for detailed proofs.

Theorem 3.1. *Let $d \in \mathbb{D}$. Then the direct problem (2.1) has a unique weak solution $u \in S^{\beta}(\Omega_T)$. Moreover, for a.e $t \in [0,T]$ there exist some constants $c, C > 0$ such that*

$$\frac{\partial^{\beta}\|u\|^2}{\partial t^{\beta}} + c\,\|u\|^2_{H_0^1(\Omega)} \leq C\,\left[\|f\|^2 + \|g_1\|^2_{L^2(\Gamma_1)} + \|g_2\|^2_{L^2(\Gamma_2)}\right].$$

Theorem 3.2. *Suppose that a sequence of coefficients $\{d_m\} \subset \mathbb{D}$ converges pointwise in $[0,\infty)$ to a function $d \in \mathbb{D}$. Then, the sequence of solutions $u_m := u(x,y,t;d_m)$ converges to the solution $u := u(x,y,t;d) \in S^{\beta}(\Omega_T)$, where $u := u(x,y,t;d)$ denotes the solution of the direct problem (2.1) for a given coefficient $d \in \mathbb{D}$.*

Next, we prove an existence theorem for a solution to the inverse problem. There are two methods in the literature to prove existence of the solution of inverse problems. The first method is called the monotonicity method based on the continuity and the monotonicity of the input-output mapping. The second method is called quasi-solution method based on minimizing an error functional between the output data and the additional data. We adopt the quasi-solution approach to the inverse problem under consideration. For this purpose, we show that the cost functional defined by (2.10) is continuous and we construct a compact subset of the class of the admissible coefficients.

Theorem 3.3. *Assume that a sequence of coefficients $\{d_m\} \subset \mathbb{D}$ converges pointwise in $[0,\infty)$ to a function $d \in \mathbb{D}$. Then $\left|I(d_m) - I(d)\right| \to 0$ as $n \to \infty$.*

Proof. Let $\{d_m\} \subset \mathbb{D}$ be a sequence of coefficients that converges pointwise in $[0,\infty)$ to a function $d \in \mathbb{D}$, $u_m := u(x,y,t;d_m)$ and $u := u(x,y,t;d)$. Then we have

$$\begin{aligned}\left|I(d_m) - I(d)\right| = \Bigg| &\int_0^T \int_{\Gamma_3} \left|u_m - \hat{g}_1(x,t)\right|^2 dx\,dt - \int_0^T \int_{\Gamma_3} \left|u - \hat{g}_1(x,t)\right|^2 dx\,dt \\ &+ \int_0^T \int_{\Gamma_4} \left|u_m - \hat{g}_2(y,t)\right|^2 dy\,dt - \int_0^T \int_{\Gamma_4} \left|u - \hat{g}_2(y,t)\right|^2 dy\,dt\Bigg|.\end{aligned} \tag{3.1}$$

For the first two terms in (3.1), by using $\left|\|a\| - \|b\|\right| \leq \|a-b\|$, we have :

$$
\begin{aligned}
&\left| \int_0^T \int_{\Gamma_3} \left| u_m - \hat{g}_1(x,t) \right|^2 dx\, dt - \int_0^T \int_{\Gamma_3} \left| u - \hat{g}_1(x,t) \right|^2 dx\, dt \right| \\
&= \left| \left\| u_m - \hat{g}_1(x,t) \right\|^2_{L^2(\Gamma_{3T})} - \left\| u - \hat{g}_1(x,t) \right\|^2_{L^2(\Gamma_{3T})} \right| \\
&\leq \left\| u_m - u \right\|_{L^2(\Gamma_{3T})} \times \left(\left\| u_m - \hat{g}_1(x,t) \right\|_{L^2(\Gamma_{3T})} \right. \\
&\qquad \left. + \left\| u - \hat{g}_1(x,t) \right\|_{L^2(\Gamma_{3T})} \right) \\
&\leq \left\| u_m - u \right\|_{L^2(\partial\Omega\times(0,T))} \times \left(\left\| u_m - \hat{g}_1(x,t) \right\|_{L^2(\Gamma_{3T})} \right. \\
&\qquad \left. + \left\| u - \hat{g}_1(x,t) \right\|_{L^2(\Gamma_{3T})} \right) \\
&\leq C \left\| u_m - u \right\|_{L^2(\Omega_T)} \times \left(\left\| u_m - \hat{g}_1(x,t) \right\|_{L^2(\Gamma_{3T})} \right. \\
&\qquad \left. + \left\| u - \hat{g}_1(x,t) \right\|_{L^2(\Gamma_{3T})} \right) \\
&\leq \tilde{C} \left\| u_m - u \right\|_{S^\beta(\Omega_T)} \times \left(\left\| u_m - \hat{g}_1(x,t) \right\|_{L^2(\Gamma_{3T})} \right. \\
&\qquad \left. + \left\| u - \hat{g}_1(x,t) \right\|_{L^2(\Gamma_{3T})} \right),
\end{aligned}
\tag{3.2}
$$

where we used the Trace and Sobolev embedding theorems, and $C, \tilde{C} > 0$ are constants. We conclude that the first two terms in (3.1) tend to zero as $n \to \infty$. Similarly, we can prove that the last two terms in (3.1) go to zero as $n \to \infty$. This completes the proof.

□

The conditions (2.2) and (2.3) arise in the solvability of the direct problem (2.1) and can be found in some papers, for example see the condition $H3$ in [52]. In virtue of Theorem 3.3, it is natural to construct a compact set of admissible coefficients in $C(I)$. For this reason, in addition to assumptions (2.2) and (2.3) we assume that there is a subset $\mathbb{D}_c$ of $\mathbb{D}$ which is equicontinuous, i.e. $\mathbb{D}_c \subset \mathbb{D}$ and for every $\epsilon > 0$ there exists a $\delta > 0$ such that if $d \in \mathbb{D}_c, s_1, s_2 \in l$ and $|s_1 - s_2| < \delta$, then $|d(s_1) - d(s_2)| < \epsilon$. By following Theorem 3 in [53] it can be proved that $\mathbb{D}_c$ is compact. Then, we prove the following existence theorem by using compactness of $\mathbb{D}_c$ and Theorem 3.3 :

Theorem 3.4. *The inverse problem has at least one quasi-solution in the set of admissible coefficients $\mathbb{D}_c$.*

The following theorem shows that the input-output operator defined by (2.8) is a compact operator.

Theorem 3.5. [49] *Let the conditions* (2.2) *and* (2.3) *hold. Then the input-output operator defined by* (2.8) *is a compact operator.*

Since nonlinear equations with compact operators are ill-posed [54], the inverse problem under consideration is an ill-posed problem. The following example shows that there exists a sequence $\{d_n\}$ such that $u(x,y,t;d_n),\ (x,y,t)\in\Gamma_{1T}$ and $u(x,y,t;d_n),\ (x,y,t)\in\Gamma_{2T}$ converges to zero as $n\to\infty$, but $d_n\to\infty$ as $n\to\infty$.

Example: For $d_n(u)=n^2$, $\beta=1/2$ and $f_n(x,t)=\dfrac{8x^3y^2t^{3/2}}{3\sqrt{\pi}n^5}-\dfrac{2xt^2}{n^3}(3y^2+x^2)$, the inverse problem (2.1) becomes

(3.3)
$$\begin{cases} \dfrac{\partial^\beta u}{\partial t^\beta}=(n^2u_x)_x+(n^2u_y)_y+\dfrac{8x^3y^2t^{3/2}}{3\sqrt{\pi}n^5}-\dfrac{2xt^2}{n^3}(3y^2+x^2),(x,y,t)\in\Omega_T,\\ u(x,y,t)=0,(x,y,t)\in\Gamma_{3T}\cup\in\Gamma_{4T},\\ -n^2u_y(x,y,t)=-\dfrac{2}{n^3}x^3t^2,(x,y,t)\in\Gamma_{1T},\\ -n^2u_x(x,y,t)=-\dfrac{3}{n^3}y^2t^2,(x,y,t)\in\Gamma_{2T},\\ u(x,y,0)=0,(x,y)\in\bar{\Omega}. \end{cases}$$

It can easily be verified that the function $u_n(x,y,t;d_n)=\dfrac{x^3y^2}{n^5}t^2$ is the solution of the corresponding direct problem. Obviously, $u_n(x,1,t;d_n)$ and $u_n(1,y,t;d_n)$ converge to zero as $n\to\infty$, but $d_n(u)\to\infty$ as $n\to\infty$.

4. Numerical solution of the direct problem

In this section, we introduce the methodology used for solving the direct problem numerically. The main idea is to convert the fractional partial differential equation into a system of fractional ordinary differential equations using the method of lines and vectorization and solve the resulting system of fractional ordinary differential equations. In addition to using the classical method of lines, we adopt the operator approach to approximate derivatives, which reduces computational and memory demand of the algorithm. We first illustrate the methodology over a one dimensional heat equation. For this purpose, we consider the following one dimensional problem:

$$\begin{cases} \dfrac{\partial u}{\partial t}=k\dfrac{\partial^2u}{\partial x^2},\ x\in(0,1),\ t\in(0,1),\\ u(x,0)=h(x),\ x\in(0,1),\\ u(0,t)=f(t),\ u(1,t)=g(t),\ t\in(0,1). \end{cases}$$

For a given positive integer M, let $x_i=i\Delta x$ for $i=0,1,2,\cdots,M$ with $\Delta x=1/M$. Also let $u_i(t)$ denote the approximation of the solution at the node (x_i,t) for $i=0,1,2,\cdots,M$, where $u_0(t)=f(t)$ and $u_M(t)=g(t)$. We approximate the given equation by the following system of ordinary differential equations for u_i's:

$$\begin{cases} \dfrac{du_i}{dt}=k\dfrac{u_{i+1}-2u_i+u_{i-1}}{\Delta x^2},\ t\in(0,1),\ i=1,\cdots,M-1,\\ u_i(0)=h(x_i),\ i=1,\cdots,M-1. \end{cases}\tag{4.1}$$

Given the vector of approximate solutions at each node without boundaries, $[u_i] = [u_1, u_2, \cdots, u_{M-1}]$, we define the left and right shift operators as

$$LS([u_i]) = [u_{i+1}] \text{ and } RS([u_i]) = [u_{i-1}],\ i = 0, 1, 2, \cdots, M-1. \tag{4.2}$$

Then, the system of ordinary differential equations given in equation (4.1) can be written in the following form :

$$\left[\frac{du_i}{dt}\right] = \frac{LS([u_i]) - 2[u_i] + RS([u_i])}{\Delta x^2}, \tag{4.3}$$

with $\left[\frac{du_i}{dt}\right] = \left[\frac{du_1}{dt}, \frac{du_2}{dt}, \cdots, \frac{du_{M-1}}{dt}\right]$ is being the vector of time derivatives at the discretized nodes. To illustrate how we generalize the shift-operator approach to higher dimensional partial differential equations, we consider the following two dimensional problem:

$$\begin{cases} \dfrac{\partial u}{\partial t} = \dfrac{\partial^2 u}{\partial x^2} + \dfrac{\partial^2 u}{\partial y^2} + f(x, y, t), (x, y, t) \in \Omega_T, \\ u(x, y, 0) = h(x, y), (x, y) \in \Omega, \\ u(x, y, t) = g(x, y, t), (x, y) \in \partial\Omega,\ t \in (0, 1). \end{cases} \tag{4.4}$$

Let $x_i = i\Delta x,\ i = 0, \cdots, M$ and $y_j = j\Delta y,\ j = 0, 1, 2, \cdots, N$ with $\Delta x = 1/M$ and $\Delta y = 1/N$. Also, let $u_{ij}(t)$ denotes the solution at point (x_i, y_j) at a time $t \in (0, 1)$, where $u_{0j} = g(0, y_j, t)$, $u_{Mj} = g(1, y_j, t)$, $u_{i0} = g(x_i, 0, t)$, $u_{iN} = g(x_i, 1, t)$. Then, the centered difference approximation of the time derivative at point (x_i, y_j) would be

$$\frac{du_{ij}}{dt} = \frac{u_{i+1j} - 2u_{ij} + u_{i-1j}}{\Delta x^2} + \frac{u_{ij+1} - 2u_{ij} + u_{ij-1}}{\Delta y^2} + f(x_i, y_j, t),$$

with $i = 1, \cdots, M-1$ and $j = 1, \cdots, N-1$. This approximation can be vectorized by first defining the solution matrix at the interior points $[u_{ij}] = u(x_i, y_j)$ with $i = 1, \cdots, M-1$ and $j = 1, \cdots, N-1$. We define the left and right shift operators on the matrix $[u_{ij}]$ of solution approximations at the interior points as follows:

$$LS([u_{ij}]) = [u_{i+1j}] \text{ and } RS([u_{ij}]) = [u_{i-1j}],$$

with $i = 1, \cdots, M-1$ and $j = 1, \cdots, N-1$. Then the matrices of the centered difference approximations to the first order derivatives can be expressed as follows:

$$[u_{xij}] = \frac{LS([u_{ij}]) - RS([u_{ij}])}{2\Delta x}, \tag{4.5}$$

$$[u_{yij}] = \frac{LS([u_{ij}]') - RS([u_{ij}]')}{2\Delta y}, \tag{4.6}$$

where $[a_{ij}]'$ denotes the transpose of the matrix $[a_{ij}]$. The matrices of the centered difference approximations to the second order derivatives, $[u_{xxij}]$, $[u_{yyij}]$, and $[u_{xyij}]$ can be obtained by applying LS and RS operators to the matrices of the first order derivative approximations given in (4.5) and (4.6). Then, (4.4) can be expressed in matrix form as follows:

$$\left[\frac{du_{ij}}{dt}\right] = [u_{xxij}] + [u_{yyij}] + [f(x_i, y_j, t)], \tag{4.7}$$

with initial condition matrix $[u_{ij}(0)] = [h(x_i, y_j)]$ of size $M - 1 \times N - 1$.

Next, we consider the following time-fractional problem:

$$\begin{cases} \dfrac{\partial^\beta u}{\partial t^\beta} = f(x,y,t,u,u_x,u_y,u_{xx},u_{yy},u_{xy}), (x,y,t) \in \Omega_T, \\ u(x,y,0) = h(x,y)\ (x,y) \in \Omega, \\ u(x,y,t) = g(x,y,t), (x,y) \in \partial\Omega,\ t \in (0,1). \end{cases} \tag{4.8}$$

Then, vectorized method of line approach described in examples above results in the following difference approximation:

$$\left[\frac{\partial^\beta u_{ij}}{\partial t^\beta}\right] = f([x_{ij}],[y_{ij}],t,[u_{ij}],[u_{xij}],[u_{yij}],[u_{xxij}],[u_{yyij}],[u_{xyij}])], \tag{4.9}$$

with $[u_{ij}(0)] = [h(x_i,y_j)]$ $[x_{ij}] = [x_i]_{1\times M-1} \otimes [1]_{N-1\times 1}$ and $[y_{ij}] = [y_j]_{N-1\times 1} \otimes [1]_{M-1\times 1}$, where $\otimes$ denotes the Kronecker matrix product. This is a system of nonlinear fractional ordinary differential equations which we solve using a Matlab implementation of the Adam-Bashfort-Moulton(ABM) type predictor-corrector method given in the work [60]. Detailed convergence and stability analysis are considered both in their subsequent work [61] and in the work [62]. In [61], the authors conclude that if the solution under consideration is sufficiently smooth, the method has uniform convergence of order h^2 for $\beta > 1$, and of order $h^{1+\beta}$ for $\beta < 1$, respectively. It is further shown by numerical examples that, these bounds are strict and can not be improved. The ABM is a Predict-Evaluate-Correct-Evaluate(PECE) type method. That is, for the approximation at the time nodes t_k, and corresponding approximations, $y_j \cong y(t_k)$ at each k_{th} step, there are two approximations computed for the next node, namely, predictor, $yp(t_{k+1})$, and using the predictor, the corrector approximation $yc(t_{k+1})$ is obtained and used in the calculation. The error is obtained by finding the difference of predictor and corrector approximations. There are two main advantages of using PECE type compared to the classical equivalent-order explicit methods. First benefit in using a PECE type algorithm is the increased accuracy and stability, see [55, 58, 62] and [59, Ch. 6]. For fractional ordinary differential equations, it was shown that the stability and accuracy remains high compared to equivalent-order numerical methods, see [60]-[62]. The second advantage of using the PECE type numerical approximation is the fact that, this method can assume variable time steps that reduces the computational cost of the approximation. The method can control the time steps by using the difference between the corrector and the predictor approximations. When the difference is smaller than the desired level of accuracy with the current time step, this is used as an indication that the solver is in a non-stiff area, and time steps are increased in an adaptive manner. The idea of combining the Method of Lines approach to reduce the given fractional partial differential equation to a system of fractional ordinary differential equations and using shift operators in the evaluation of the right-hand side of the PDE can prove to be useful in terms of memory and computation compared to similar operator approaches such as that of Podlubny's intuitive matrix operator approach, see [56, 57], depending on the problem under consideration. In terms of memory, the Method of Lines approach uses matrices of size $M \times N$. Whereas in Podlubny's Matrix Operator approach, the matrices under consideration are of size $M \times N \times K$ where K is the number of mesh points in t direction used in the calculation. So the Method of Lines approach improves the

TABLE 1. Absolute error between u_{num} and u_{exact} for $\beta = 0.7$

M(=N)	Absolute Error	CPU Time (Seconds)
20	0.2347	17.22
10	0.0847	8.49
5	0.021	6.14

TABLE 2. Absolute error between u_{num} and u_{exact} for $\beta = 0.6$

M(=N)	Absolute Error	CPU Time (Seconds)
20	0.3135	23.139
10	0.0949	8.397
5	0.0232	6.12

memory demand of the calculations. But this improvement in the memory comes at the cost of calculation of the right-hand side function at each time step. However, Podlubny's matrix operator approach can also face the computational challenges depending on the complexity of the fractional partial differential equation. This is because, the method requires solving nonlinear algebraic matrix equation of very high dimensions. Hence, the very nature of the question under consideration is the sole factor in choosing the numerical method to apply.

The first series of the numerical simulations is related to numerical solution of the direct problem. For this purpose, the function $u(x, y, t) = tx^2y^2$ is taken to be the analytic solution of the equation $\dfrac{\partial^\beta u}{\partial t^\beta} = (d(u)u_x)_x + (d(u)u_y)_y + f(x, y, t)$, with the function $d(u) = 1 + u$ and appropriately chosen source function $f(x, y, t)$. The boundary conditions are found from the trace of the function $u(x, y, t) = tx^2y^2$ on Ω. First, we check the difference between the numerical solution u_{num} and the exact solution $u_{\text{exact}} = u(x, y, t) = tx^2y^2$. The absolute error between u_{num} and u_{exact} is defined by $\|u_{\text{num}} - u_{\text{exact}}\|_\infty$, where $\|\cdot\|_\infty$ denotes the sup norm, which is taken over all x, y, t where $x \in [0, 1], y \in [0, 1]$ and $t \in [0, 0.3]$. The software is simulated for different values of the system parameters to see their effect on the absolute error and the simulation time. Time step is taken $\Delta t = 10^{-5}$. We note that decreasing the time step increases the simulation time and has almost no effect in the computations. However, there is a subtle relation the number of time nodes and x , y nodes. Increasing $\Delta t = 10^{-5}$ when $t \in [0, 0.3]$ affects the stability of the simulation when higher number of x, y nodes is desired. We simulated the solution for $M = N = 5$, $M = N = 10$ and $M = N = 20$ for $\beta = 0.6$ and $\beta = 0.7$. We see the results with computation times in Table 1 and Table 2. We observe that $M = N = 5$ serves the best time and the least absolute error. Also, it appears that as β increases towards 1, the absolute error decreases. Hence, the time step and number of discretization nodes for the remaining simulations are chosen to be seemingly optimal values of 10^{-5} and $M = N = 5$.

Next, we consider the ill-posedness of the inverse problem. A problem is called to be well-posed in the Hadamard sense if the solution exists, unique and depends continuously on the input data. Failure to comply any of the mentioned properties makes the given problem ill-posed. To show that the inverse problem under

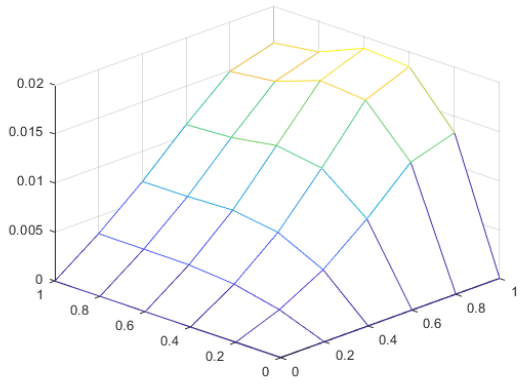

FIGURE 1. Ill-posedness of the inverse problem: the graph of the difference between the numerical solutions corresponding to $a_1(u) = u + 1$ and $a_2(u) = u + 3$.

consideration is ill-posed, we simulate the direct problem for $a_1(u) = 1 + u$ and $a_2(u) = 3+u$. The functions $u_1(x, y, 1)$ and $u_2(x, y, 1)$ are found from the numerical solution. Figure 1 shows that the graph of the difference $abs(u_1(x, y, 1)-u_2(x, y, 1))$ where we see the solutions on both Γ_{3T} and Γ_{4T} are very close to each other with an absolute difference less than 0.02.

5. Numerical solution of the inverse problem

We assume that for a fixed β, the following problem has the solution $\tilde{u}(x, y, t)$ for the specific functions $\tilde{d}, f(x, y, t), g_1(x, t)$ and $g_2(y, t)$. In the inverse problem, our goal is to try to find the function $\tilde{d}$ when only $\tilde{u}(x, 1, t)$ and $\tilde{u}(1, y, t)$ are known about the solution $\tilde{u}$ while the boundary conditions and $f(x, y, t)$ are known and fixed. The boundaries are same as in (2.1). In our experiments, first we fix our solution $\tilde{u}(x, y, t)$ as tx^2y^2 and the specific function $d(u)$ beforehand. By using them we find $g_1(x, t)$, $g_2(x, t)$ exactly and $f(x, y, t)$ numerically. Now $g_1(x, t)$, $g_2(x, t)$ and $f(x, y, t)$ at hand, we take $\tilde{u}(1, y, t) = ty^2$ and $\tilde{u}(x, 1, t) = tx^2$ as additional conditions for the inverse problem and we try to find $d(u)$. When doing this, we set up the following error functional for each function d as in (2.11):

$$I(d) := \int_0^T \int_0^1 \left| u(x, y, t; d) - \tilde{u}(x, 1, t) \right|^2 dx\, dt + \int_0^T \int_0^1 \left| u(x, y, t; d) - \tilde{u}(1, y, t) \right|^2 dy\, dt,$$

where $u(x, y, t; d)$ denotes the solution of the direct problem for the function d. It is clear that $I(\tilde{d}) = 0$. Thus, we expect to find $\tilde{d}(u)$ as the minimizer of the error function. We carry out the experiment for noise-free data and noisy data. For noisy data, we add the noise $0.1\phi_1(x, t)$ and $0.1\phi_2(x, t)$ to $g_1(x, t)$ and $g_2(x, t)$ respectively where $\phi_1(x, t)$ and $\phi_2(x, t)$ take values in the form of $0.1 \times m(x, t)$ where m takes random values from $[-1, 1]$. We will use polynomials to approximate the minimum

$\tilde{d}$ in the light of Theorem 3.2. For $n > 0$, we assume $d(u) = d_n u^n + \cdots + d_0$. Thus, $I(d)$ is a function of the vectors $(d, d_0) \in \mathbb{R}^{n+1}$ where $d = d = (d_n, \cdots d_1)$. We apply the BGFS Method, a Quasi-Newton Method, to minimize the function which will require computing the gradient of the function $I(d)$. The BGFS method approximates the Hessian of the error function with a cubic line search procedure in each step. For further reading, see [26]. We choose the stopping criteria for the algorithm as $||\nabla I(d)|| < 10^{-6}$. The integration in $I(d)$ is calculated by the trapezoid rule.

In the experiments, in accordance with observations in Section 4, we take $\beta = 0.7$ for the order of fractional time derivative, $M = N = 5$ are used to make a meshgrid for x and y on $[0, 1] \times [0, 1]$ and time step is taken as $\triangle t = 10^{-5}$ and $T = 0.3$. Also we take the variable $d(u)$ as a third degree polynomial. Hence, $I(d)$ is treated as a function of three variables. In the tables, the initial points denoted by d_{final} are chosen to be close to the coefficients of the second degree Taylor polynomial of $\tilde{d}(u)$, a random number between 0 and 1 is added or subtract to each component. In the tables, we provide the value of $I(d)$ for the final d, i.e., d_{final} the algorithm reached and the relative error between the solution of the direct problem, i.e, u_{final} for the d_{final} and $u = tx^2y^2$ is given by

$$\text{Relative Error} := \frac{||u_{\text{final}}(x, y, t) - tx^2y^2||_\infty}{||tx^2y^2||_\infty},$$

where $||\cdot||_\infty$ is estimated by the maximum value of the function on the meshgrid on $[0, 1] \times [0, 1] \times [0, 0.3]$.

The inverse problem is an ill posed problem and it is sensitive to the noise dramatically. To deal with the noisy data, we use Tikhonov regularization in the error functional and define it as :

$$\begin{aligned} I(d) := &\int_0^T \int_0^1 \left| u(x, y, t; d) - \tilde{u}(x, 1, t) \right|^2 dx\, dt \\ &+ \int_0^T \int_0^1 \left| u(x, y, t; d) - \tilde{u}(1, y, t) \right|^2 dy\, dt + \lambda ||d||_e^2, \end{aligned} \tag{5.1}$$

where $||\cdot||_e$ is the Euclidean norm. We run the algorithm for different regularization parameter λ with the same initial values and present the best results according to the relative error.

Experiment 1. The correct $d(\cdot)$ is $\tilde{d}(u) = 2\sin(u) + \cos(u)$, whose second degree Taylor polynomial is $-0.5u^2 + 2u + 1$. Table 3 and 4 show the results for the noise-free and noisy data, respectively. Table 5 shows the best results for different values of the regularization parameter λ.

Experiment 2. The correct $d(\cdot)$ is $\tilde{d}(u) = u^2 + u + 1$. Table 6 and 7 show the results for the noise-free and noisy data respectively. Table 8 shows the best results for different values of the regularization parameter λ.

Experiment 3. The correct $d(\cdot)$ is $\tilde{d}(u) = e^u$ whose second degree Taylor polynomial is $0.5u^2 + u + 1$. Table 9 and 10 show the results for the noise-free and noisy data respectively. Table 11 shows the best results for different values of the regularization parameter λ.

TABLE 3. Results for noise-free data for $\tilde{d}(u) = 2\sin(u) + \cos(u)$

d_{initial}			d_{final}			$I(d_{\text{final}})$	Relative Error
-0.27408	2.0855	1.0987	-0.30691	1.9416	1.0172	6.5695e-08	0.0053729
-0.32929	2.2625	0.73813	-0.41756	1.9666	1.0105	2.3175e-08	0.0032792
-1.4234	2.7303	0.27877	-0.56634	2.0006	1.0014	3.0948e-10	0.00055506
-0.93021	1.5114	1.1068	-0.79997	2.0539	0.98705	4.4387e-08	0.0039033
-0.68482	1.4215	0.34624	-0.60656	2.0101	0.99864	9.2876e-10	0.00053536
0.40488	2.2373	1.4942	-0.58484	2.0048	1.0003	2.2985e-10	0.00029774
0.47975	2.4588	0.22095	-0.58776	2.0056	0.99998	2.7193e-10	0.00034198
-0.06113	1.0369	1.715	-0.58706	2.0054	1.0001	2.6604e-10	0.00034775
-0.38888	1.4532	0.096279	-0.35227	1.9509	1.0152	4.5877e-08	0.0044349
-0.75806	2.5211	1.8909	-0.79146	2.0521	0.9875	4.1074e-08	0.0037083
-0.76221	1.3759	0.80219	-0.63609	2.0172	0.99653	3.2795e-09	0.0008257
-0.27825	1.6326	1.5	-0.19536	1.9171	1.0234	1.3041e-07	0.0076122
-0.79668	2.0377	1.9047	-0.74601	2.0417	0.99027	2.5509e-08	0.0028553
-0.92417	1.0867	1.6177	-0.68659	2.0283	0.99378	1.0782e-08	0.0017539

TABLE 4. Results for noisy data for $\tilde{d}(u) = 2\sin(u) + \cos(u)$

d_{initial}			d_{final}			$I(d_{\text{final}})$	Relative Error
-0.27408	2.0855	1.0987	-0.3141	1.9232	1.0344	0.0020018	0.0052846
-0.32929	2.2625	0.73813	-0.42473	1.9484	1.0275	0.0020017	0.0032272
-1.4234	2.7303	0.27877	-0.67733	2.0063	1.0119	0.0020016	0.0021874
-0.93021	1.5114	1.1068	-0.80617	2.0373	1.0027	0.0020016	0.0037943
-0.68482	1.4215	0.34624	-0.61309	1.9932	1.0148	0.0020016	0.0021119
0.40488	2.2373	1.4942	-0.69746	2.0106	1.0109	0.0020016	0.0022959
0.47975	2.4588	0.22095	-0.70218	2.012	1.0104	0.0020016	0.0023236
-0.06113	1.0369	1.715	-0.70344	2.0122	1.0104	0.0020016	0.0023527
-0.38888	1.4532	0.096279	-0.35922	1.9326	1.0323	0.0020017	0.0043445
-0.75806	2.5211	1.8909	-0.79917	2.0341	1.0044	0.0020016	0.0037813
-0.76221	1.3759	0.80219	-0.64273	1.9991	1.0135	0.0020016	0.002096
-0.27825	1.6326	1.5	-0.20201	1.899	1.0403	0.0020018	0.0075475
-0.79668	2.0377	1.9047	-0.75291	2.0236	1.0072	0.0020016	0.0029034
-0.92417	1.0867	1.6177	-0.69291	2.0101	1.0107	0.0020016	0.0022322

TABLE 5. Results for noisy data for $\tilde{d}(u) = 2\sin(u) + \cos(u)$ with regularization parameter

d_{initial}			d_{final}			$I(d_{\text{final}})$	Relative Error	λ
-0.32929	2.2625	0.73813	-0.41297	1.936	1.0355	0.0020067	0.0037234	10^{-6}
0.40488	2.2373	1.4942	0.229	1.7102	1.1339	0.0020458	0.021791	10^{-5}
-0.68482	1.4215	0.34624	0.22395	1.4118	1.3433	0.0024042	0.083568	10^{-4}
-0.92417	1.0867	1.6177	0.16702	1.1677	1.3914	0.0055819	0.31648	10^{-3}

TABLE 6. Results for noise-free data for $\tilde{d}(u) = u^2 + u + 1$

d_{initial}			d_{final}			$I(d_{\text{final}})$	Relative Error
1.8143	1.5688	1.1067	0.98685	1.0027	0.99947	1.8662e-10	0.00021487
1.2435	1.4694	0.038102	1.0944	0.981	1.0043	8.5119e-09	0.0014074
1.9293	0.9881	1.0046	0.98892	1.0026	0.9992	1.3021e-10	0.00018254
0.8034	1.1622	1.8173	0.81833	1.0366	0.99164	3.1636e-08	0.0027013
1.3517	1.1656	1.2599	1.3088	0.9365	1.0151	9.1374e-08	0.0046914
1.8308	1.602	0.19993	0.98007	1.0051	0.99838	5.4332e-10	0.00039664
1.5853	0.73703	1.4314	0.9837	1.0037	0.99902	3.2042e-10	0.00029842
0.082806	1.6892	1.1818	1.0041	0.99907	1.0003	1.7019e-11	6.6238e-05
0.2428	0.54946	1.1455	1.0075	0.99842	1.0004	5.5279e-11	0.00011151
0.24627	0.91618	0.86393	1.0279	0.99108	1.0038	1.5989e-09	0.00061966
1.0759	0.84762	1.5499	1.1222	0.97718	1.0042	1.438e-08	0.0017248
1.054	0.17418	0.85505	1.1964	0.96141	1.0082	3.6805e-08	0.0028801
0.22083	1.9961	0.37794	1.0108	0.99797	1.0004	1.1477e-10	0.00014608
0.065989	0.92182	1.351	1.0119	0.9973	1.0008	1.4633e-10	0.00018962

TABLE 7. Results for noisy data for $\tilde{d}(u) = u^2 + u + 1$

d_{initial}			d_{final}			$I(d_{\text{final}})$	Relative Error
1.8143	1.5688	1.1067	0.87821	1.0042	1.0132	0.0020016	0.0015718
1.2435	1.4694	0.038102	1.0871	0.96223	1.0227	0.0020017	0.0023355
1.9293	0.9881	1.0046	0.86725	1.0068	1.0123	0.0020016	0.00169
0.8034	1.1622	1.8173	0.81146	1.0196	1.0086	0.0020016	0.002464
1.3517	1.1656	1.2599	1.3018	0.9178	1.0335	0.0020018	0.0050523
1.8308	1.602	0.19993	0.86061	1.0086	1.0118	0.0020016	0.0018171
1.5853	0.73703	1.4314	0.87637	1.0045	1.0131	0.0020016	0.001589
0.082806	1.6892	1.1818	0.88511	1.0027	1.0136	0.0020016	0.001566
0.2428	0.54946	1.1455	0.37128	1.1072	0.98935	0.0020019	0.0089087
0.24627	0.91618	0.86393	0.89739	0.99902	1.0151	0.0020016	0.0016656
1.0759	0.84762	1.5499	1.1151	0.95842	1.0225	0.0020017	0.0023623
1.054	0.17418	0.85505	1.1896	0.94251	1.0266	0.0020017	0.0032631
0.22083	1.9961	0.37794	0.89089	1.0018	1.0136	0.0020016	0.0015688
0.065989	0.92182	1.351	0.91539	0.99126	1.0192	0.0020016	0.0019827

TABLE 8. Results for noisy data for $\tilde{d}(u) = u^2 + u + 1$ with regularization parameter

	d_{initial}			d_{final}		$I(d_{\text{final}})$	Relative Error	λ
0.8034	1.1622	1.8173	0.79386	1.0152	1.0136	0.0020043	0.0023183	10^{-6}
1.3517	1.1656	1.2599	0.23178	1.0905	1.0144	0.0020249	0.0095046	10^{-5}
0.22083	1.9961	0.37794	0.15297	0.96968	1.0883	0.0022225	0.025866	10^{-4}
1.3517	1.1656	1.2599	0.11759	0.81796	1.0163	0.0039331	0.1176	10^{-3}

TABLE 9. Results for noise-free data for $\tilde{d}(u) = e^u$

d_{initial}			d_{final}			$I(d_{\text{final}})$	Relative Error
0.90181	1.5752	1.4868	0.79218	0.94905	1.0105	5.6575e-08	0.0046883
0.57597	1.0598	0.56414	0.54444	0.99668	1.0006	1.4739e-10	0.000262
0.73992	0.76522	1.4468	0.78835	0.95044	1.0099	5.4814e-08	0.0047249
0.62332	0.64684	0.69365	0.67086	0.97351	1.0048	1.5113e-08	0.0024087
0.26005	1.0154	0.48923	0.25222	1.0548	0.98759	7.5481e-08	0.0059219
0.45035	0.83101	0.20517	0.45166	1.0131	0.99813	7.8171e-09	0.0022299
1.4027	1.6491	1.6443	0.53726	0.99922	0.99945	6.6822e-11	0.00026575
1.4448	1.7317	0.62139	0.51571	1.0057	0.99697	1.064e-09	0.00053638
-0.40005	1.2963	0.060998	0.5487	0.99689	1	9.9924e-11	0.00019071
0.13075	0.25531	1.8759	0.32007	1.0428	0.98936	4.4431e-08	0.0045091
0.88974	1.1835	0.41296	0.81012	0.94438	1.0121	6.5201e-08	0.0048764
0.40355	1.7802	1.4709	0.28431	1.0486	0.98887	5.966e-08	0.0052538
-0.44205	0.070614	1.8443	0.55639	0.99609	0.99981	2.7998e-10	0.00020745
-0.45613	0.22429	0.80524	0.55508	0.99551	1.0004	2.3236e-10	0.00026031

TABLE 10. Results for noisy data for $\tilde{d}(u) = e^u$

d_{initial}			d_{final}			$I(d_{\text{final}})$	Relative Error
0.90181	1.5752	1.4868	0.78517	0.93079	1.0288	0.0020018	0.0050131
0.57597	1.0598	0.56414	0.53751	0.97834	1.019	0.0020016	0.0022175
0.73992	0.76522	1.4468	0.78169	0.93207	1.0283	0.0020018	0.0051061
0.62332	0.64684	0.69365	0.66409	0.9552	1.0231	0.0020017	0.0028501
0.26005	1.0154	0.48923	0.24532	1.0365	1.0059	0.0020017	0.0055843
0.45035	0.83101	0.20517	0.44478	0.99464	1.0166	0.0020016	0.0023482
1.4027	1.6491	1.6443	0.40493	1.0054	1.0124	0.0020016	0.0024947
1.4448	1.7317	0.62139	0.41451	1.0035	1.013	0.0020016	0.0022539
-0.40005	1.2963	0.060998	0.42752	1.001	1.0135	0.0020016	0.0021903
0.13075	0.25531	1.8759	0.3134	1.0244	1.0078	0.0020016	0.0041734
0.88974	1.1835	0.41296	0.80315	0.92604	1.0305	0.0020018	0.0051862
0.40355	1.7802	1.4709	0.27712	1.0303	1.0072	0.0020017	0.0049314
-0.44205	0.070614	1.8443	0.43707	0.99816	1.0147	0.0020016	0.0022583
-0.45613	0.22429	0.80524	0.43069	1.0003	1.0138	0.0020016	0.002201

TABLE 11. Results for noisy data for $\tilde{d}(u) = e^u$ with regularization parameters

d_{initial}			d_{final}			$I(d_{\text{final}})$	Relative Error	λ
0.57597	1.0598	0.56414	0.52797	0.97607	1.0214	0.0020039	0.0023258	10^{-6}
0.26005	1.0154	0.48923	0.22214	1.0051	1.0289	0.002023	0.012937	10^{-5}
0.98925	0.54908	0.46717	0.13735	0.92151	1.0695	0.002208	0.051983	10^{-4}
0.36803	1.0811	0.76951	0.10825	0.7698	0.96251	0.003772	0.27405	10^{-3}

Since the algorithm is based on approaching $d(u)$ with polynomials and the error function is a function of three variables, the third degree Taylor polynomials of the correct $d(u)$'s are expected to be attained by the algorithm for each initial point.

In all experiments with noise-free data, we observe that the algorithm finds the linear coefficients of the target Taylor polynomial for almost all initial points, while it mostly fails to reach the nonlinear coefficient, i.e., the coefficient of u^2 of the target Taylor polynomial for most of the initial points. However, the coefficients of the final $d(u)$'s with the least relative errors almost matches the coefficient of u^2 of the target Taylor polynomial. The relative error for the solution u corresponding to each final polynomial $d(u)$ in all of the experiments is observed to fluctuate between 0.0001 and 0.007 roughly. Another observation for noise-free experiments is that the more $I(d)$ is, the more the relative error for the corresponding u naturally.

In all experiments that are carried out with noisy data, there is a significant behavior in the error function: $I(d_{\text{final}})$ stays around 0.002 for almost all initial points. The relative error for all initial points and experiments fluctuate between 0.001 and 0.009. So the relative error increases up to 10 times. One observation about the experiments with noisy data is that even though the linear coefficients of d_{final} are more distanced from the linear coefficients of expected Taylor polynomials, they still seem to accumulate around the expected linear coefficients. The nonlinear coefficients look far from the expected.

The experiments show that the linear part of the $d(u)$ behaves robust against the noise. This is most probably due to the constraints imposed by the method used in the solution of the direct problem. Note that we have a stable solution for t in $[0, 0.3]$ with $\triangle = 10^{-5}$.

For the noisy data, we apply the Tikhonov regularization. The regularization parameters are very close to zero, i.e. 10^{-7} and less seem to work well. Also, it has been observed that the linearization of $d(u)$ is robust against the noise. It appears that the robustness of the linear part increases as β approaches to 1. In the experiments with $\beta = 0.6$, (not shown in this article) the results have shown that the error increases more and final points are found to be further from the expected. So, we can conclude that the problem becomes more ill-posed as β decreases. We also note that one can use also trust region methods to minimize the error functional. Indeed, some tests have been carried out with trust region method and the BGFS method. A significant difference in the computation time has been observed between two optimization methods. For this reason, the BGFS method has been chosen.

6. Concluding Remarks

In the solution of the direct problem, we observe that as the order of fractional time derivative approaches to 1, the numerical solution approximates the exact solution better. Also, it appears that there is a subtle relation between the size interval and time step. We observe that $M = N = 5$ serves the best time and the least absolute error. The numerical results of the experiments show that solving the inverse problem stated in this article using the error functional with the help of polynomials and solving the direct problem with line search method works well. However, the computational constraints resulting from the discussion of the solution of the direct problem makes the problem a bit restrictive on the mesh-grid and time interval. The experiments with noise-free data verifies the theoretical results, i.e., the existence of a quasi-solution.The experiments with noisy data show that the linear part of the $d(u)$ behaves robust against the noise. Also, as β gets far from 1, the problem tends to be more ill-posed.

References

[1] D. Campos, J. Fort, V. Mendez. Propagation through fractal media: The Sierpinski gasket and the Koch curve. *Europhysics Letters*, 68(6), 769-775, 2004. 1

[2] O. Y. Dinariyev. The pressure build-up curve for a fractal cracked porous medium. Linear theory. *J. Appl. Math. Mech..*, 58, 755-758, 1994.

[3] D. H. N. Anh, K. H. Hoffmann, S. Seeger, S. Tarafdar. Diffusion in disordered fractals. *Europhysics Letters*, 70(1), 109-115, 2005.

[4] C. Essex, M. Davison, C. Schulsky, A. Franz, K. Hoffmann. The differential equation describing random walks on the Koch curve. *J. of Physics A: Math. Gen.*, 34, 8397-8406, 2001.

[5] S. Fomin, V. Chugunov, T. Hashida. Non-Fickian mass transport in fractured porous media. *Advances in Water Resources*, 34(2), 205-214, 2011.

[6] M. Giona, H. E. Roman. Fractional diffusion equation on fractals: one-dimensional case and asymptotic behavior. *J. Phys. A: Math. Gen.*, 25, 2093-2105, 1992.

[7] R. R. Nigmatullin. The realization of the generalized transfer equation in a medium with fractal geometry. *Phys. Stat. Sol. (b)*, 133, 425-430, 1986.

[8] B. O'Shaughnessy, I. Procaccia. Diffusion on fractals. *Phys. Rev. A*, 32, 3073-3083, 1985.

[9] R. T. Sibatov, V. V. Uchaikin. Fractional differential approach to dispersive transport in semiconductors. *Uspekhi Fizicheskih Nauk*, 179(10), 1079-1104, 2009.

[10] V. V. Uchaikin. The Fractional Derivatives Method. *Artishok Press, Ul'yanovsk*, 2008. 1

[11] A. A. Kilbas, H. M. Srivastava and J. J. Trujillo. Theory and Applications of Fractional Differential Equations. *Elsevier, Amsterdam*, 2006. 1

[12] I. Podlubny. Fractional Differential Equations. *Academic Press, San Diego*, 1999. 1

[13] D. Del-Castillo-Negrete, B. A. Carreras and E. Lynch. Front dynamics in reaction-diffusion systems with Lévy flights: a fractional diffusion approach. *Phys. Rev. Lett.*, 91:018302(4), 2003. 1

[14] S. Fomin, V. Chugunov and T. Hashida. Application of Fractional Differential Equations for Modeling the Anomalous Diffusion of Contaminant from Fracture into Porous Rock Matrix with Bordering Alteration Zone. *Transport in Porous Media*, 81:187-205, 2010.

[15] S. Fomin, V. Chugunov and T. Hashida. Mathematical Modeling of Anomalous Diffusion in Porous Media. *Fract. Differ. Calc.*, 1(1):1-28, 2011.

[16] G. Li, D. Zhang, X. Jia and M. Yamamato. Simultaneous inversion for the space-dependent diffusion coefficient and the fractional order in the time fractional diffusion equation. *Inverse Problems*, 29:065014, 2013.

[17] R. Metzler and J. Klafter. The random walks guide to anomalous diffusion: a fractional dynamics approach. *Physics Reports*, 339, 1-77, 2000. 1

[18] R. R. Nigmatulin. To the theoretical explanation of the universal response. *Phys. Stat. Sol.(b)*, 123, 739-745, 1984. 1

[19] R. R. Nigmatulin. The realization of the generalized transfer equation in a medium with fractal geometry. *Phys. Stat. Sol. (b)*, 133, 425-430, 1986. 1

[20] S. Fomin, V. Chugunov, T. Hashida. Mathematical modeling of anomalous diffusion in Porous media. *Fractional Differential Calculus*, 1, 1-28, 2011. 1

[21] L.A. Richards. Capillary conduction of liquids through porous mediums. *Journal of Applied Physics*, 1(5), 318-333, 1931. 1

[22] L. Plociniczak. Analytical studies of a time-fractional porous medium equation. Derivation, approximation and applications. *Commun. Nonlinear Sci. Numer. Simulat.*, 24, 169-183, 2015. 1, 1

[23] Y. Pachepsky, D. Timlin, W. Rawls. Generalized Richards equation to simulate water transport in unsaturated soils. *Journal of Hydrology*, 272, 3-13, 2003. 1

[24] D. N. Gerasimov, V. A. Kondratieva, O. A. Sinkevich. An anomalous non-self-similar infiltration and fractional diffusion *Physica D: Nonlinear Phenomena*, 239(16), 1593-1597, 2010. 1

[25] E. Gerolymatou, I. Vardoulakis, R. Hilfer. Modeling infiltration by means of a non-linear fractional diffusion model. *J. Phys. D: Appl. Phys.*, 39(18), 4104-4110, 2006.

[26] J. Nocedal, S. Wright, *Numerical optimization*, Springer Science & Business Media (2006). 5

[27] S. Shen, F. Liu, Q. Liu, V. Anh. "Numerical simulation of anomalous infiltration in porous media. *Numer. Algorithm*, 68(3), 443-454, 2015. 1

[28] E. N. de Azevedo, P L. de Souza, R. E. de Souza, M. Engelsberg. Concentration-dependent diffusivity and anomalous diffusion: A magnetic resonance imaging study of water ingress in porous zeolite. *Physical Review E*, 73, 011204, 2006. 1

[29] W. L. Vargas, L. E. Palacio, D. M. Dominguez. Anomalous transport of particle tracers in multidimensional cellular flows. *Physical Review E*, 67, 026314, 2003. 1

[30] L. Plociniczak. Approximation of the Erdelyi-Kober operator with applications to the time-fractional porous medium equation. *Siam J. Appl. Math.*, 74(4), 1219-1237, 2014. 1

[31] L. Plociniczak, H. Okrasinska Approximate self-similar solutions to a nonlinear diffusion equation with time-fractional derivative. *Physica D*, 261, 85-91, 2013. 1

[32] H. Sun, M. M. Meerschaert, Y. Zhang, J. Zhu, W. Chen. A fractal Richards equation to capture the non-Boltzmann scaling of water transport in unsaturated media. *Advances in Water Resources*, 52, 292-295, 2013. 1

[33] J. Cheng, J. Nakagawa, M. Yamamoto, T. Yamazaki. Uniqueness in an inverse problem for a one-dimensional fractional diffusion equation. *Inverse Problems*, 25, 115-131, 2009. 1

[34] B. Jin, W. Rundell. An inverse problem for a one-dimensional time-fractional diffusion problem. *Inverse Problems*, 28, 075010, 2012.

[35] J. J. Liu, M. Yamamoto. A backward problem for the time-fractional diffusion equation *Applicable Analysis*, 89, 1769-1788, 2010.

[36] K. Sakamoto, M. Yamamoto. Inverse source problem with a final overdetermination for a fractional diffusion equation. *Math. Controls Rel. Fields.*, 4, 509-518, 2011.

[37] K. Sakamoto, M. Yamamoto. Initial value/boundary value problems for fractional diffusion-wave equations and applications to some inverse problems. *J. Math. Anal. Appl.*, 382, 426-447, 2011.

[38] X. Xu, J. Cheng, M. Yamamoto. Carleman esimate for a fractional diffusion equation with half order and application. *Applicable Analysis*, 90, 1355-1371, 2011.

[39] M. Yamamoto, Y. Zhang. Conditional stability in determining a zeroth-order coefficient in a halforder fractional diffusion equation by a Carleman estimate. *Inverse Problems*, 28, 105010, 2012.

[40] Y. Zhang, X. Xu. Inverse source problem for a fractional diffusion equation. *Inverse Problems*, 27, 035010, 2011.

[41] G. Li, X. Zhang, M. Yamamoto. Simultaneous inversion for the space-dependent diffusion coefficient and the fractional order in the time fractional diffusion equation. *Inverse Problems*, 29, 065014, 2013.

[42] S. Tatar, R. Tinaztepe, S. Ulusoy. Determination of an unknown source term in a space-time fractional diffusion equation. *J. Fract. Calc. Appl.*, 6(2), 94-101, 2015.

[43] S. Tatar, R. Tinaztepe, S. Ulusoy. Simultaneous inversion for the exponents of the fractional time and space derivatives in the space-time fractional diffusion equation. *Applicable Analysis.*, 95, 1-23, 2016.

[44] S. Tatar, S. Ulusoy. A uniqueness result in an inverse problem for a space-time fractional diffusion equation. *Electron. J. Differ. Equ.*, 258, 1-9, 2013.

[45] S. Tatar, S. Ulusoy. An inverse source problem for a one-dimensional space-time fractional diffusion equation. *Applicable Analysis*, 94(11), 2233-2244, 2015.

[46] N. H. Tuan, L. D. Long, S. Tatar. Tikhonov regularization method for a backward problem for a inhomogeneous time-fractional diffusion equation *Applicable Analysis*, https://doi.org/10.1080/00036811.2017.1293815. 1

[47] S. Tatar, S. Ulusoy. Analysis of Direct and Inverse Problems for a Fractional Elastoplasticity Model. *Filomat*, 31(3), 699-708, 2017. 1

[48] S. Tatar, R. Tinaztepe, M. Zeki. Numerical Solutions of Direct and Inverse Problems for a Time Fractional Viscoelastoplastic Equation. *Asce Journal of Engineering Mechanics*, 143(7), 04017035, 2017. 1

[49] S. Tatar, S. Ulusoy. An inverse problem for a nonlinear diffusion equation with time-fractional derivative. *J. Inverse Ill-Posed Probl.*, 25(2), 185-193, 2017. 1, 3, 3.5

[50] J.R. Canon, P Duchateau. An inverse problem for a nonlinear diffusion equation. *Siam J. Appl. Math.*, 39(2), 272-289, 1980. 1

[51] P Duchateau. Monotonicity and Uniqueness Results in Identifying an Unknown Coefficient in a Nonlinear Diffusion Equation. *Siam J. Appl. Math.*, 41(2), 310-323, 1981. 1

[52] J. Manimaran, L. Shangerganesh, A. Debbouche, J.-C. Cortes A time-fractional HIV infection model with nonlinear diffusion. *Results in Physics.*, 25, 104293, 2021. 3

[53] Y.H Ou, A. Hasanov and H.L Liu. Inverse coefficient problems for nonlinear parabolic differential equations. *Acta Mathematica Sinica, English Series*, 24(10), 1617-1624, 2008. 3
[54] H. W. Engl, K. Kunisch, A. Neubauer Convergence rates for Tikhonov regularisation of non-linear ill-posed problems Inverse Problems 5 (1989), 523–540. 3
[55] Atkinson K.: An Introduction to Numerical Analysis. Wiley, New York (1989). 4
[56] Podlubny I.: Matrix approach to discrete fractional calculus. *Fractional Calculus and Applied Analysis*, 3(4): 359–386, 2000. 4
[57] Podlubny I., Chechkin A. V., Skovranek T., Chen Y. Q, Vinagre B.: Matrix approach to discrete fractional calculus II: partial fractional differential equations. *Journal of Computational Physics*, 228(8): 3137–3153, 2009. 4
[58] Iserles, A.: Numerical Analysis of Differential Equations Cambridge University Press, Cambridge (1996). 4
[59] E. Hairer E. and Wanner G.: Solving Ordinary Differential Equations II: Stiff and Differential-Algebraic Problems, Springer, Berlin, (1991). 4
[60] Diethelm K. Freed A. D.: The Frac PECE subroutine for the numerical solution of differential equations of fractional order, in: S. Heinzel, T. Plesser (Eds.), Forschung und Wissenschaftliches Rechnen (1998), Gessellschaft fur Wissenschaftliche Datenverarbeitung, Gottingen, pp. 57–71, (1999). 4
[61] Diethelm K., Ford N. J., Freed A. D.: Detailed error analysis for a fractional Adams method, Numer. Algorithms 36 (1), 31–52, 2004. 4
[62] Garrappa R.: On linear stability of predictor-corrector algorithms for fractional differential equations, Internat. J. Comput. Math. 87 (10), 2281–2290, 2010. 4

(Mustafa Zeki)
Department of Mathematics,
American University of Middle East,
Kuwait
Email address: mustafa.zeki@aum.edu.kw

(Ramazan Tinaztepe)
Department Basic Sciences
Deanship pf Preparatory year and supporting studies
Imam Abdulrahman Bin Faisal University
Dammam, KSA
Email address: ttinaztepe@iau.edu.sa

(Salih Tatar)
Department of Mathematics & Computer Science ,
College of Science,
Alfaisal University,
Riyadh, KSA
Email address: statar@alfaisal.edu

(Süleyman Ulusoy)
Department of Mathematics and Natural Sciences,
Faculty of Arts and Sciences,
American University of Ras Al Khaimah,
RAK, UAE
Email address: suleyman.ulusoy@aurak.ac.ae